ISSN 1560-8034, 1605-6582 (On-line), SPQEO, 2019. V. 22, N 1. P. 5-10.

Semiconductor physics

Electronic, structural and paramagnetic properties of magnesium telluride

J.O. Akinlami[1*], M.O. Omeike[2] and A.J. Akindiilete[1]

[1]*Federal University of Agriculture, Department of Physics, Abeokuta, P.M.B 2240, Abeokuta, Nigeria*
[2]*Federal University of Agriculture, Department of Mathematics, Abeokuta, P.M.B 2240, Abeokuta, Nigeria*
**Corresponding author e-mail: johnsonak2000@yahoo.co.uk*

Abstract. This study has examined the ground-state electronic, structural and, in addition, paramagnetic properties of semiconductor MgTe in its zinc blende phase by using the density functional theory (DFT). Exchange-correlation potentials have been approximated with the Projected Augmented Wave (PAW) Generalized Gradient Approximation (GGA). From the calculated lattice parameter, we determined the bulk modulus and first pressure derivative. Also, reported are other ground state properties: density of states (DOS), band structure, projected DOS (PDOS) and magnetic properties. A direct large band-gap of 2.358 eV was observed from the band structure that has close concurrence with former reported values. Although this value is also smaller than the reported experimental values, it is the closest of all the calculated values. The magnetic state of the compound was observed to be paramagnetic in the ground state.

Keywords: $A^{II}B^{IV}$ semiconductor, magnetic properties, electronic structure, density of states.

doi: https://doi.org/10.15407/spqeo22.01.5
PACS 71.20.Mq, 75.50.Pp

Manuscript received 20.10.18; revised version received 29.01.19; accepted for publication 20.02.19; published online 30.03.19.

1. Introduction

Compounds of the alkaline earth chalcogenides (AECs) are reportedly to be of great relevance in technology with its application not limited only to catalysis or microelectronics [1, 2]. This has motivated several research works both theoretically and experimentally. They are also very germane in fabricating luminous devices [2-6]. Magnesium telluride is II-VI semiconductor and also AEC.

In MgTe, the valence band has some lowered maxima, which consequently increase their fundamental band gap [7]. MgTe has been reported to have the possibility of exhibiting several crystallographic phases such as cubic and hexagonal states. While the cubic phase can be the rock salt (B1) and zinc blende (B3), the hexagonal structure exhibits wurtzite (B4), and NiAs (B8) phases, respectively. In some experimental studies, MgTe has been predicted to have a stable hexagonal wurtzite structure in its ground state [4, 8-11] and for the possibility of experiencing a phase transition from this wurtzite phase to the NiAs one, its pressure should be increased between 1…3.5 GPa [13, 21]. However, some local density approximation (LDA) calculations predicted the NiAs phase to have the stable structure of MgTe in its ground state [14-16].

Drief *et al.* [15] used full potential-linear-augmented plane-wave (FP-LAPW) of the LDA scheme, in studying MgTe properties (structural, electronic and optical) both in the B3 and B8 phases. Also, the full-potential linear muffin-tin orbital method (FP-LMTO) local density approximation was used by Rached *et al.* [17] to calculate the electronic band structures of MgTe as well as its total energies in its B8 and high pressure phases, respectively. Their results that also include the pressure at which the compound undergoes phase transition from B8 phase to the CsCl phase were found to be consistent with previous works.

Lattice dynamics of MgTe under its various structural phases (B1, B3, B8 and B4) was investigated by Gokhan [18] using the DFT [19, 20] within plane-wave pseudo-potential method and the generalized gradient approximation (GGA) functional [19, 20]. His results showed that MgTe exist in the ground state as a fourfold wurtzite structure, which agrees well with both experimental and computational studies.

This work aim is to provide worthwhile contributions to the several existing works, moreover a good validation to the works of Gokhan Gokoglu [18, 21] where MgTe was studied with the GGA formalism. Therefore, our primary objective is to use the density functional theory (DFT) within projected augmented wave (PAW) of the Perdew–Burke–Ernzerhof (PBE) [22, 23] exchange correlation for GGA to study magnesium telluride in its zinc blende phase (B3), since PAW (GGA) calculations have been accepted to give better and accurate calculations than the LDA method [22, 23] that was widely used by previous researchers [15, 17, 24-26].

It is also worthy of note that while few studies of B3 phase of MgTe existed within the GGA formalism, PAW GGA studies has only been made once for the compound. To the best of our knowledge, calculation of the magnetic state of this compound being reported for the first time.

2. Method of calculations

The calculations in this work were done with the plane wave self-consistent field (PWSCF) code contained in the Quantum ESPRESSO package [27-29]. The Hohenberg and Kohn equations [30, 31] within Perdew–Burke–Ernzerhof (PBE) [22, 23] in the density functional theory were solved using the PAW GGA exchange correlation for the MgTe compound. The ultrasoft pseudo-potentials [32] of PAW were used for both the magnesium and telluride atoms.

For the magnesium atom, the valence state was taken as $3s^2$, while for the tellurium atom $5s^25p^4$ was considered as the valence one. The Brillouin zone sampling was performed automatically with 6×6×6 k-point mesh in the Monkhorst and Pack scheme [33]. This k-point yields 55 k-points, which was employed in plotting the band structure.

Using the plane wave bases, wave functions were expanded by setting up the kinetic energy cut-off value to 70 Ry, while 280 Ry was used as the charge density cut-off resulting from high ionicity characteristic of the compound. Self-consistent computations were performed for MgTe to the point of convergence with these values. The Davidson diagonalization method was iteratively used for solving Kohn–Sham equations keeping the convergence threshold of the energy as $1\cdot10^{-9}$ Ry.

The lattice parameter with the bulk modulus, pressure derivative, volume and the ground state energy were obtained from the output data sets fitted to the Murnaghan equation of state [35]. The pressure can be calculated from the equation:

$$P=\left(\frac{B_0}{B_0'}\right)\left(\left(\frac{V_0}{V}\right)^{B_0'}-1\right). \quad (1)$$

We will be able therefore to deduce the volume from the equation (1) above as follows:

$$V(P)=V_0\left(1+P\left(\frac{B_0'}{B_0}\right)^{\frac{-1}{B_0'}}\right), \quad (2)$$

where P, V, V_0, B_0, B_0' are the pressure, volume, equilibrium volume, bulk modulus and bulk modulus pressure derivative, respectively.

These values were found to agree well with previous calculations on MgTe. Using the non-logarithmic scale, the charge density was also plotted, while the magnetization [41] for the compound defined as M was calculated in accord with the equation

$$M=\chi_m H, \quad (3)$$

where χ_m is the magnetic susceptibility given as

$$\chi_m=\mu_r-1. \quad (4)$$

3. Results and discussion

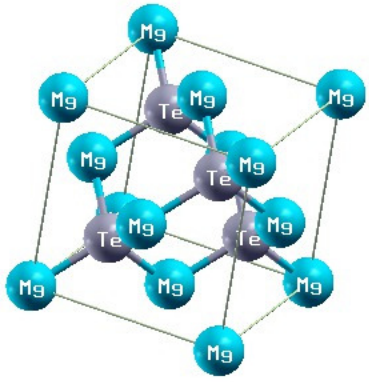

Fig. 1. Magnesium telluride crystal structure in the conventional zinc blende phase (B3) exhibiting the face-centered cubic (FCC) structure.

Table 1. Comparison of the obtained ground state structural parameters for magnesium telluride with the previous works.

Parameter	This work	Theoretical data taken from							Experimental data	
		[18]	[15]	[21]	[36]	[37]	[12]	[38]	[35]	[39]
a	12.31	12.337	12.079	12.306	12.174	12.066	12.32	12.10	12.132	12.019
B_0	33.2	33.8	38.0	34.1	38.0	39.0	34.3	38		
B_0'	3.73	4.31	3.79	4.30	3.96		4.31	4.01		

Notes. Lattice parameter a in a.u., B_0 in GPa, B_0' is dimensionless.

Table 2. The calculated band-gap energy compared with theoretical and experimental works

	Band-gap energy (eV)
This work	2.358
Theory [12]	2.31
Theory [40]	2.29
Theory [21]	2.32
Experiment [10]	3.50

The structural properties of MgTe obtained in this work have been compared with the previous studies (theoretical and experimental) shown in Table 1. The ground state equilibrium properties (equilibrium lattice constant, bulk modulus (B_0) alongwith its pressure derivative (B_0') was obtained by fitting the calculated total energies to the Murnaghan equation of state. The pressure for each volume was calculated analytically from the first derivative of the Murnaghan equation according to volume equations (1), (2). The calculated lattice parameter 12.31 a.u. agrees well with the previous works by Gokoglu, 2010, Gokoglu *et al*., 2009, and Guo *et al*., 2013, where the GGA formalism was used, whereas other results where the LDA formalism have been adopted gave a value closer to the experimental values. This observation is accounted for by the over-estimation of the GGA potentials. On the other hand, the bulk modulus and pressure derivative, 33.2 and 3.73 GPa, respectively, are the lowest of all other computed values. The bulk modulus and pressure derivative of this study agree with the works of Drief *et al*., 2004, and Gokoglu, 2010, even though the former adopted LDA formalism and the latter – GGA formalism. This validates the uniqueness of the PAW GGA formalism over LDA.

The MgTe band structure crystalizing in the zinc blende phase shown in Fig. 2 was calculated later following the high symmetry points of the Brillouin zone. The Fermi energy level was positioned at the zero point on the energy scale level with the symmetry position shown via the vertical lines. MgTe depicts a direct band gap semiconductor from the maxima of the valence band as well as the minima of the conduction band occurring at the Γ-point, respectively. This band structure agrees well with the previously reported results from experimental and theoretical works shown in Table 2. Although there is a little difference in our band-gap value when comparing with other computed values, this difference exists as a result of the pseudo-potential used. Even though, the band-gap value predicted by Gokoglu *et al*., 2009 is the closest to our calculated band-gap, this work still gives the closest value to the experimental value, which is also a justification on the accuracy of the PAW GGA formalism.

The total density of states (DOS) representing the number of electrons in the available states per unit volume per unit energy is shown in Fig. 3. Total DOS also shows the same trend of large band-gap semiconductor (between 0.13 and 2.48 eV) as we have in the band structure (Fig. 2). Also DOS has its peak

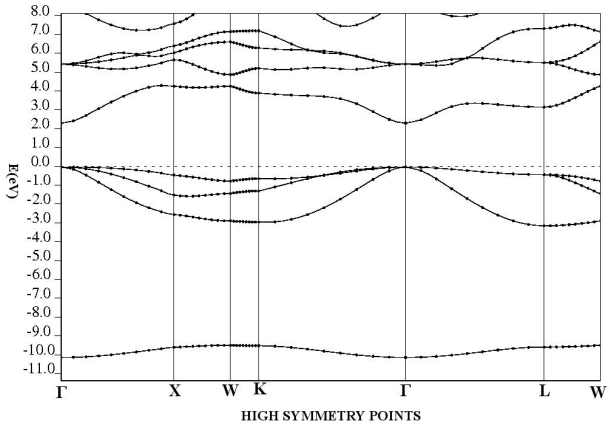

Fig. 2. Band structure of MgTe in B3 phase.

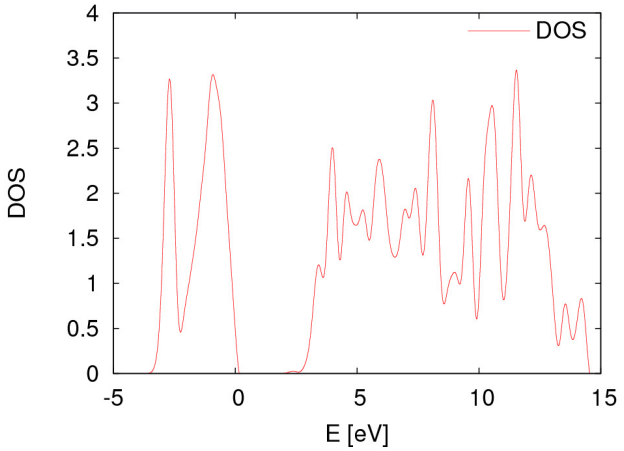

Fig. 3. DOS of MgTe in B3 phase.

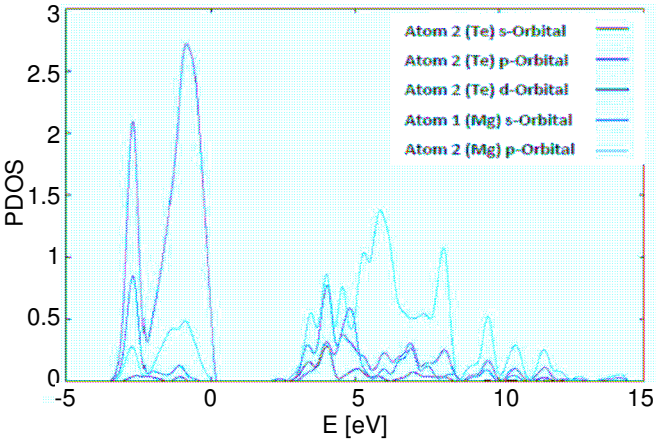

Fig. 4. Partial density of states of MgTe in the zinc blende phase (B3).

location between 11.02 and 13.22 eV. The DOS energy spectra show that charges are only distributed between the ranges of –3.46 to 14.57 eV.

Partial DOS of MgTe was plotted in Fig. 4 depicting the major contribution of orbitals in the band structure. PDOS presents different layers of sinusoidal curves with each curve denoting a particular orbital of the

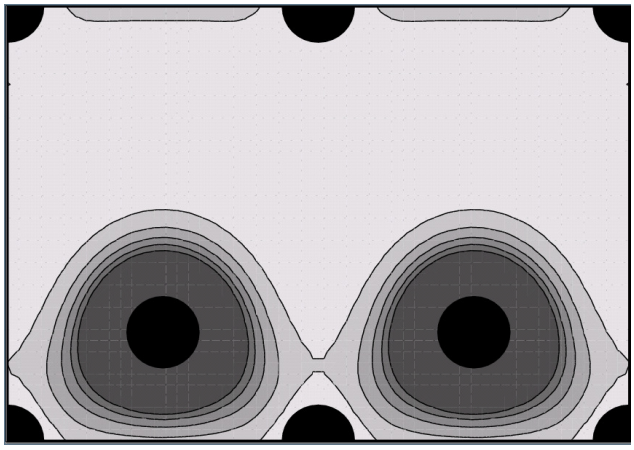

Fig. 5. Charge density of MgTe in the phase B3. Black circle – Mg atom, grey circle – Te atom.

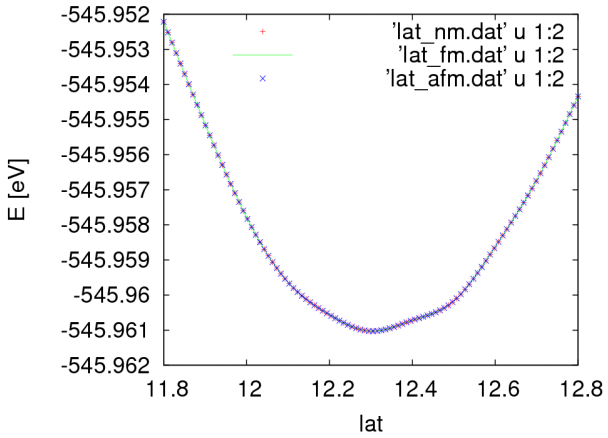

Fig. 6. Total energy against lattice parameters of the non-magnetic (+), ferromagnetic (—) and antiferromagnetic (×) magnesium telluride.

constituent atoms. The first region represents the valence bands occurring within the energy range of –3.39 and 0.16 eV, which comprises Mg 3*s*, Mg 3*p*, Te 5*s* and Te 5*p* orbitals. The lower part is largely dominated by the Mg 3*s*, 3*p* and Te 5*s* states with the upper part being dominated by the Te 5*p* states. The second region representing the conduction band occurring the energy range between 2.64 and 14.43 eV. This part is majorly dominated by Mg 3*s* and Mg 3*p* states with participation of Te 5*p* and 5s orbitals in the lower region. However, the energy band-gap value of the compound is contributed by Te 5*p* orbital as the maxima of the valence band at 0.16 eV and Mg 3*s* orbital as the minima of the conduction band at 2.51 eV.

The dynamic charges of zinc blende representing the bond existent between the atoms of MgTe were predicted from the charge density plot. To account for the bonding type, whether ionic or covalent, we present the real space for the electronic charge densities of MgTe in the plane (110) shown in Fig. 5. The figure revealed the existence of covalence bond evidenced from the partial sharing of electron. However, it is worth to note that this covalent bond is not strong, since we only observe a weak sharing in the middle of the atoms as shown above. Upon the introduction of spin into the compound and calculating the lattice parameter for every change in the kinetic energy cutoff, we obtain various data sets for the non-magnetic MgTe, ferromagnetic MgTe as well as its antiferromagnetic state. The plot of the corresponding lattice parameters against the respective ground-state energy helps to reveal its magnetic status. The lattice optimization plot for these three different magnetic states all fall on the same point as shown in Fig. 6. This is an indication of the ground state magnetic state of the compound revealing MgTe to be non-magnetic. Furthermore, the output data for the magnetization of the compound in its ferromagnetic and antiferromagnetic states revealed that the total and absolute magnetization for MgTe are both zero. Therefore, we conclude that MgTe is a paramagnetic compound.

4. Conclusion

We have examined ground-state electronic, structural and paramagnetic properties of the magnesium telluride with DFT. We obtained structural properties and the electronic properties that compared well with experimental studies and recent theoretical calculations. A direct large band-gap of 2.358 eV was observed from the band structure. The magnetization revealed in MgTe in the ground state is paramagnetic.

Acknowledgements

Authors are grateful to Professor G.A. Adebayo and Dr P.O. Adebambo of Department of Physics, Federal University of Agriculture, Abeokuta, Nigeria for their immense contributions.

References

1. Wang M.W., Phillips M.C., Swenberg J.F., Yu E.T., McCaldin J.O., & McGill T.C. (1993). *n*-CdSe/*p*-ZnTe based wide band-gap light emitters: Numerical simulation and design. *J. Appl. Phys.* 1993. **73**, No 9. P. 4660–4668.
2. Pandey R., Sivaraman S. Spectroscopic properties of defects in alkaline-earth sulfides. *J. Phys. Chem. Solids*. 1991. **52**, issue 1. P. 211–225.
3. Zimmer H.G., Winze H. and Syassen K. High-pressure phase transitions in CaTe and SrTe. *Phys. Rev. B*. 1985. **32**. P. 4066–4070.
4. Zachariasen W. Über die Kristallstruktur des Magnesiumtellurids. *Z. Phys. Chem*., Stoechiom. Verwandtschaftsl. 1927. **128**. P. 417.
5. Asano S., Yamashita N. and Nakao Y. Luminescence of the Pb^{2+}-ion dimer center in CaS and CaSe phosphors. *phys. status solidi* (*b*). 1978. **89**, No. 2. P. 663–673. doi:10.1002/pssb.2220890242.

6. Nakanishi Y., Ito T., Hatanaka Y., Shimaoka G. Preparation and luminescent properties of SrSe:Ce thin films. *Appl. Surf. Sci.* 1993. **65–66**. P. 515–519.
7. Wei S.H., Zunger A. Role of metal *d* states in II-VI semiconductors. *Phys. Rev. B*. 1988. **37**. P. 8958.
8. Kuhn A., Chevy A., Naud M.J. Preparation and some physical properties of magnesium telluride single crystals. *J. Cryst. Growth*. 1971. **9**. P. 263–265.
9. Klemm W., Wahl K. Notiz Über das Magnesiumtellurid. *Z. Anorg. Allg. Chemist*. 1951. **266.** P. 289.
10. Parker S.G., Reinberg A.R., Pinnel J.E., Holton W.C. Preparation and properties of $Mg_xZn_{1-x}Te$. *J. Electrochem. Soc*. 1971. **118**, Issue 6. P. 979.
11. Waag A., Heinke H., Scholl S., Becker C.R., Landwehr G. Growth of MgTe and $Cd_{1-x}Mg_xTe$ thin films by molecular beam epitaxy. *J. Crystal Growth*. 1993. **131**, Issue 3-4. P. 607–611.
12. Guo L., Hu G., Feng W.J., Zhang S.T. Structural, elastic, electronic and optical properties of Zinc-Blende MTe (M = Zn/Mg). *Acta Physico-Chimica Sinica.* 2013. **29**, No 5. P. 929–936.
13. Li T., Luo H., Greene R.G., Ruoff A.L., Trail S.S., DiSalvo F.J., Jr. High pressure phase of MgTe: Stable structure at STP? *Phys. Rev. Lett.* 1995. **74**, No 26. P. 5232–5235.
14. Chakrabarti A. Role of NiAs phase in pressure-induced structural phase transitions in IIA-VI chalcogenides. *Phys. Rev. B*. 2000. **62**. P. 1806.
15. Drief F., Tadjer A., Mesri D., Aourag H. First principles study of structural, electronic, elastic and optical properties of MgS, MgSe and MgTe. *Catalysis Today*. **89**, No 3. P. 343–355
16. Duman S., Bağcı S., Tütüncü H.M., and Srivastava G.P. First-principles studies of ground-state and dynamical properties of MgS, MgSe, and MgTe in the rocksalt, zinc blende, wurtzite, and nickel arsenide phases. *Phys. Rev. B.* 2006. **73**. P. 205201.
17. Rached D., Rabah M., Khenata R., Benkhettou N., Baltache H., Maachou M., Ameri M. High pressure study of structural and electronic properties of magnesium telluride. *J. Phys. Chem. Solids*. 2006. **67**, No 8. P. 1668–1673.
18. Gokhan G. First principles vibrational dynamics of magnesium telluride. *J. Phys. Chem. Solids*. 2010. **71**, No 9. P. 1388–1392.
19. Kittel C. *Introduction to Solid State Physics.* 8th Edition. John Wiley & Sons, New York, 2005. Chapters 1-3.
20. Ashcroft N.W., Mermin N.D. *Solid State Physics*. Holt, Rinehart, and Winston, NY, 1976.
21. Gokhan G., Durandurdu M., Gulseren O. First principles study of structural phase stability of wide-gap semiconductors MgTe, MgS and MgSe. *Comput. Mater. Sci*. 2009. **47**, No 2. P. 593–598.
22. Perdew J.P., Bueke K., Ernzerhof M. Generalised gradient approximation made simple. *Phys. Rev. Lett*. 1996. **77**. P. 3865.
23. Perdew J.P. and Wang Y. Pair-distribution function and its coupling-constant average for the spin-polarized electron gas. *Phys. Rev. B*. 1992. **46**. P. 12947.
24. Madu C.A., Onwuagba B.N. Electronic and structural properties of MgSe, CaSe, SrSe and BaSe. *The African Review of Physics*. 2012. **7**, No 0017. P. 171–175.
25. D. Rached, N. Benkhettou, B. Soudini, B. Abbar, N. Sekkal and M. Driz, Electronic structure calculation of magnesium chalcogenides MgS and MgSe. *phys. status solidi* (*b*). 2003. **240**, No 3. P. 565–573.
26. Varshney D., Kaurav N., Sharma U., Singh R.K. Phase transformation and elastic behavior of MgX (X = S, Se, Te) alkaline earth chalcogenides. *J. Phys. Chem. Solids*. 2008. **69**, No 1. P. 60–69.
27. Menéndez-Proupin E., Giannozzi P., Peralta J., and Gutiérrez G. Ab initio molecular dynamics study of amorphous $CdTeO_x$ alloys: Structural properties. *Phys. Rev. B*. 2009. **79**. P. 014205.
28. Giannozzi P. and 32 coauthors, QUANTUM ESPRESSO: a modular and open-source software project for quantum simulations of materials. *J. Phys. Condens. Mat.* 2009. **21**. P. 395502. doi: 10.1088/0953-8984/21/39/395502.
29. Quantum-ESPRESSO: a comm. Proj. for high-qual. DFT-based quant-simulation soft., harmonized by Paolo G. ⟨http://www.quantum-espresso.org⟩ &⟨http:// www.pwscf.org ⟩.
30. Hohenberg P. and Kohn W. Inhomogeneous electron gas. *Phys. Rev. B*. 1964. **136**. P. 864.
31. Kohn W. and Sham L.J. Self-consistent equations including exchange and correlation effects. *Phys. Rev*. 1965. **140**. P. A1133.
32. Pseudo potential ref: http:/www.quantum-espresso.org/pseudo-search-results/
33. Monkhorst H.J., Pack J.D. Special points for Brillouin-zone integrations. *Phys. Rev. B*. 1976. **13**, No 12. P. 5188.
34. Davidson E.R. The iterative calculation of a few of the lowest eigenvalues and corresponding eigenvectors of large real-symmetric matrices. *J. Computat. Phys*. 1975. **17**, Issue 1. P. 87–94.
35. Murnaghan F.D., The Compressibility of Media under Extreme Pressures. *Proc. Natl. Acad. Sci. USA*. 1944. **30**, No 9. P. 244–247.
36. Van Camp P.E., Van Doren V.E., Martins J.L. High-pressure phases of magnesium selenide and magnesium telluride. *Phys. Rev. B.* 1997. **55**. P. 775.
37. Yang J.-H., Chen S., Yin W.-J., Gong X.G., Walsh A., Wei S.-H. Electronic structure and phase stability of MgTe, ZnTe, CdTe, and their alloys in the *B*3, *B*4, and *B*8 structures. *Phys. Rev. B*. 2009. **79**. P. 245202.
38. Zhang X., Shi G., Li Z. Lattice dynamics study of magnesium chalcogenides. *Commun. Theor. Phys*. 2012. **57**. P. 295–300.

39. Hartmann J.M., Cibert J., Kany F. et al. CdTe/MgTe heterostructures: Growth by atomic layer epitaxy and determination of MgTe parameters. *J. Appl. Phys*. 1996. **80**, No 11. P. 6257–6265.
40. Flezsar A. LDA, GW, and exact-exchange Kohn–Sham scheme calculations of the electronic structure of sp semiconductors. *Phys. Rev. B*. 2001. **64**. P. 245204.
41. Satish V.K. *Material Science*, Birla Institute of Technology and Science Study Resources, India, 2010. Chapter 16.

Authors and CV

Akinlami, Johnson Oluwafemi, born in 1972, defended his Doctoral Dissertation in Physics (Theoretical Condensed Matter Physics) in 2011. Senior Lecturer at Federal University of Agriculture, Abeokuta, Ogun State, Nigeria. Authored over 30 publications. The area of his scientific interests includes optical properties of A^3B^5 and A^2B^6 compounds, photoemission study of the electronic structure of A^2B^6 compounds and and layered oxysulfide (LaO)CuS, magneto-optical properties of solids.

Omeike, Mathew Omonigho, born in 1971, defended his Doctoral Dissertation in Mathematics in 2005. Professor at Federal University of Agriculture, Abeokuta, Ogun State, Nigeria. Authored over 50 publications. The area of his scientific interests includes qualitative properties of solutions of third order delay differential equations, uniform boundedness of solutions of some third order ordinary differential equations, Generalized reduced-order hybrid combination synchronization of three Josephson junctions via back stepping technique.

Akindiilete, Ayobami Jeremiah, born in 1984, defended his Master thesis in Condensed Matter Physics in 2016. Physics Teacher at Command Day Secondary School, Ikeja, Lagos, Nigeria. The area of his scientific interests is in ab-initio calculation of the electronic, structural properties of semiconductors.